Analyst

Accepted Manuscript

ROYAL SOCIETY OF CHEMISTRY

www.rsc.org/analyst

Journal Name

RSCPublishing

ARTICLE

Near-infrared excited ultraviolet emitting upconverting phosphors as an internal light source in dry chemistry test strips for glucose sensing

T. Valta,[a,b,†] V. Kale,[b,†] T. Soukka,[b] and C. Horn[a],

Cite this: DOI: 10.1039/xoxxoooooox

Received ooth January 2012,
Accepted ooth January 2012

DOI: 10.1039/xoxxoooooox

www.rsc.org/

Upconverting phosphors are inorganic crystals with interesting optical properties, including the ability to convert infrared radiation to emission at shorter wavelengths. In this paper we present the utilization of nanosized β-$NaYF_4$:Yb^{3+},Tm^{3+}, synthesized in the presence of K^+, emitting at 365 nm under 980 nm excitation as an internal light source in glucose sensing dry chemistry test strips. The feasibility of the nanoparticles as an internal UV light source was compared to the use of an external broadband lamp. The results obtained from glucose measurement using UCNPs were in agreement with the traditional method based on measuring reflectance using an external UV light source. In addition the multiple emission peaks of UCNPs provided a possibility to use them as a control signal to account for various sources of error arising in the assay. The high penetration depth of the NIR-excitation made it also possible to excite the UCNPs through a layer of whole blood giving more freedom to the design of the optical setup.

Keywords: upconverting phosphor, glucose, ultraviolet, test strip

Introduction

Upconverting nanophosphors (UCNP) are a class of inorganic crystals capable of converting infrared excitation to emission on shorter wavelengths. The process is based on the sequential photon absorption by utilizing the long excited state lifetimes of lanthanide ions. The advances in the synthesis methods of UCNPs in recent years have made it possible to produce nanosized particles with a narrow size distribution and relatively high emission intensity (for a review see for example Haase and Schäfer[1]). In most cases these particles emit in the visible or near-IR part of the spectrum but also UV-emission has been reported, mainly from thulium and ytterbium doped $NaYF_4$ crystals[2-6]. This UV-emission has also been utilized e.g. for photoswitching of organic molecules[7, 8], photorelease of various compounds[9-14] (from small organic molecules to macromolecules) and to initiate a polymerization to coat the particles[15].

Highly photo- and thermostable UCNPs enable practically background free detection of the anti-Stokes emission with a relatively simple instrumentation, making them an ideal candidate for robust chemical sensors. So far a handful of sensors utilizing these particles have been reported. They are commonly based on the idea of using UCNPs as an internal light source in the sensing element together with an indicator compound that changes its optical properties as an analyte is introduced to the sensor. The indicator then modulates the detected emission from the UCNP by absorbing its emission[16-18] or alternatively the indicator is excited through an energy transfer and its emission is detected[19,20]. These applications utilize mostly the visible emission bands of the upconverting materials, but there is also a lot of interest towards the UV-region as e.g. nicotinamide adenine dinucleotide (NADH) is a commonly used redox-indicator with absorbance in that range. Recently an application for ethanol sensing in a solution utilizing the UV-emission of a UCNP with NADH as the indicator has been demonstrated[21].

In this paper, we describe the utilization of UV-emission of the $NaYF_4$:Yb^{3+},Tm^{3+} particles synthesized in the presence of K^+, using the UCNPs as an internal light source in disposable. single-use, glucose sensing dry chemistry test strips. The feasibility of the nanoparticles as an internal UV light source was compared to the use of an external broadband lamp used to measure reflectance.

Results and discussion

UCNP characterization

It was found that $NaYF_4$: 20 mol% Yb^{3+}, 0.5 mol% Tm^{3+} nanocrystals synthesized in the presence of 40 mol% K^+ were

excellent materials for intense ultraviolet emission (K^+ dependent UV emission spectra presented in figure 1 a). This composition was used here as a UV emission source. The phase compositions of the as-prepared products were examined by XRD. The typical diffraction patterns (Supplementary information Figure S-1) revealed that the reflection positions and intensities of the as-prepared $NaYF_4$ nanocrystals synthesized in the presence of 0 % K^+, match closely with that of hexagonal $NaYF_4$. With 40 mol% K^+ content in the synthesis, the hexagonal $NaYF_4$ phase is accompanied with a small amount of KCl. Based on the XRD, the added K^+ does not enter the $NaYF_4$ cell in any noticeable amount but it has formed an amorphous phase instead[22]. ICP-MS analysis supports this statement showing lower amount of K^+ present inside the crystals than the added quantity[22]. Addition of 40 mol% of K^+ during synthesis decreases the Na^+ concentration which results in fewer nucleation sites and thus larger $NaYF_4$ crystals (inset in Figure 1 a).

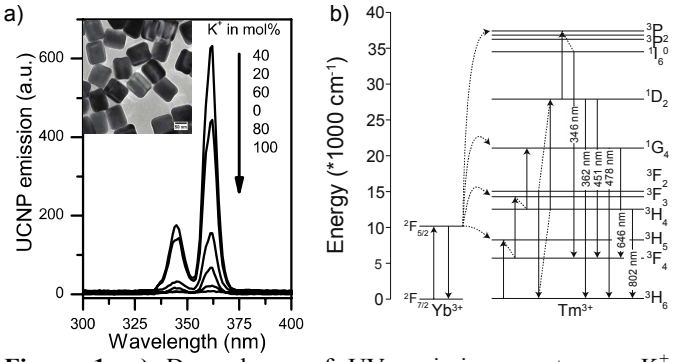

Figure 1. a) Dependence of UV emission spectra on K^+ concentration in β-$Na_{1-x}K_xYF_4$: 20% Yb^{3+}, 0.5% Tm^{3+} materials synthesized with 0-100 mol% K^+. Inset is the TEM image of 40 mol%, K^+ UCNPs. **b)** Jablonski diagram of the upconversion processes leading to the UV-emission[23].

The 362 nm emission is supposed to be 4 photon process which is the reason to lower efficiency compared to the 2 and 3 photon processes (Supplementary information Figure S-2 and Figure 1 b). Thus to enhance the efficiency of UV-emission it is required to increase the sensitization by Yb^{3+} and the Yb-Tm energy transfer. As the Na/R ratio inside the crystal decreases with the addition of 40 mol% K^+, the distance between Yb^{3+} and Tm^{3+} decreases. This is caused by the difference in the ionic radii of K^+ and Na^+ ions, which may results in more severe modification and tailor the local environment of the Yb^{3+} and Tm^{3+} ions in the crystal lattice. Therefore the radiative transition rate was enhanced, which favored the enhancement of the UC emission intensity. This 40 mol% K^+ concentration seems to be the optimal for higher UV emission.

UCNP emission on the test strips

Figure 2 shows the emission spectra of the UCNP particles (with 40 mol% K^+) measured from a glucose sensing test strip (Figure 3 a) and normalized with the 362 nm peak, measured from a dry strip, as intensity value 100. The spectrum was measured with both setups described in figure 3 b (excitation either from below or above of the strip) and how they are affected by the addition of H_2O under a 980 nm laser excitation. The decrease in the emission, after the addition of water, is caused by several factors. Most of this is caused by the quenching effect of water, the migration of particles with the sample to the lower layer and change in the optical properties of the strip.

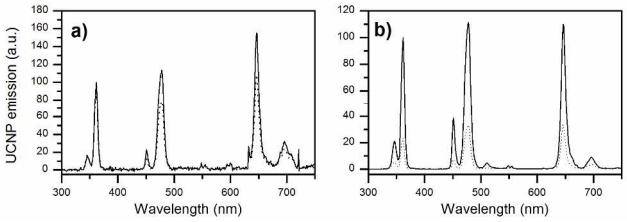

Figure 2. The UCNP emission spectrum measured from a test strip with the 980 nm excitation coming either from **a)** below or **b)** above of the strip. The solid line shows emission detected from a dry strip and dashed line the emission after addition of water on to the strip.

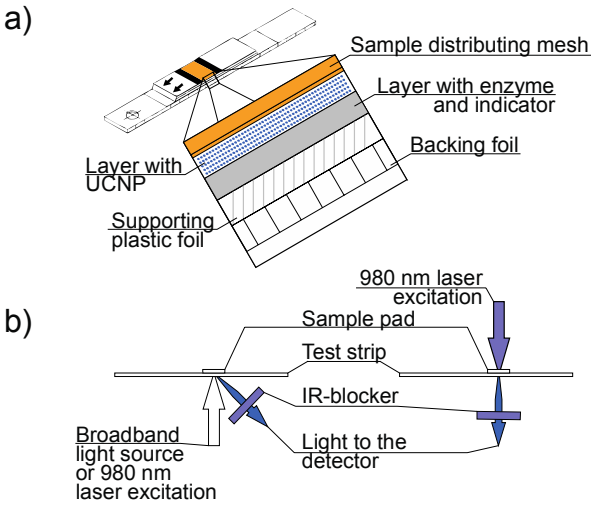

Figure 3. Diagram showing the **a)** structure of the test strips and **b)** the two optical setups used with the test strips with the light source either below or above of the strip.

The issue of quenching has been previously reported by several groups[6, 24-29] that have also achieved up to 50-fold enhancement on the emission intensity by constructing an inorganic shell without optically active ions around the UCNPs.

Glucose assay

The assay was first tested with a solution of glucose in water, using the detection setup used with the reflectance measurement, shining either a broadband light or a 980 nm laser directly below the test strip and detecting either the reflected light or the emission from the UCNP, respectively. The results from this glucose assay (Figure 4) show that the results obtained with both methods correlate well with the concentration of glucose in the sample. In terms of sensitivity and dynamic range, there is no noticeable difference between them. When the internal control of the UCNPs is omitted and only the UV-emission is used for the analysis, the standard deviations are significantly higher and the slope of the

calibration curve lower. UCNP measurement with the internal control signal improved the limit of detection from 0.93 mM to 0.49 mM compared to reflectance. The coefficient of variation in these measurements varied between 0.64-6.7 % for the UCNP with the internal control signal and 0.92-9.1 % for the reflectance measurement.

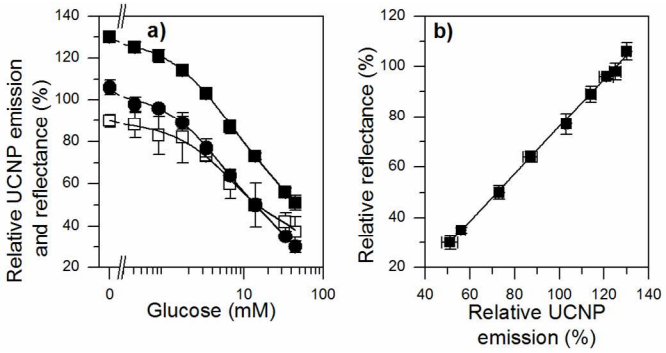

Figure 4. Results from glucose assay with light source below the strip and glucose dissolved in water as a sample. **a)** The glucose calibration curves obtained using either the emission of UCNPs (squares) or reflectance (spheres). The filled squares represent ratiometric UCNP-signal and the open squares data obtained from the UV-emission of the UCNPs alone. The bi-exponential decay curve was used for the fitting. **b)** The correlation of the relative reflectance and ratiometric UCNP emission. R^2-values of all the fittings were > 0.99. Error bars represent standard deviation.

To demonstrate the possibilities presented by the UCNPs to the design of optical setup for the readout of the test strips, we moved the excitation source to the other side of the test strips and repeated the assay using a heparinized whole blood spiked with glucose as a sample. As human blood is relatively transparent for 980 nm radiation, we were able to measure the emission of UCNPs also in this configuration. Same samples were then used also in a traditional reflectance based measurement to provide a point of comparison. The results presented in the form of relative signals from these two measurements are presented in figure 5 that is showing a good correlation between the two methods.

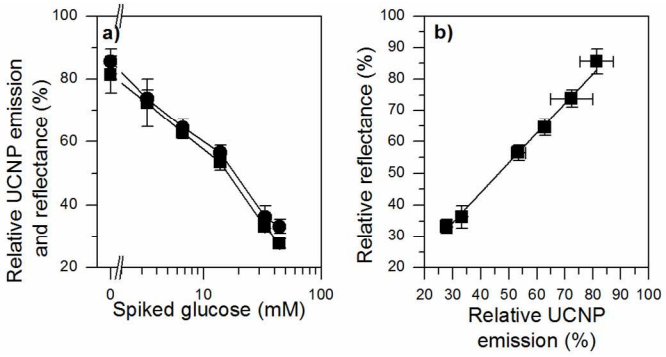

Figure 5. Results from glucose assay with whole blood as sample. The UCNPs were excited through the sample and reflectance measured from the other side. **a)** The relative signals obtained from the UCNPs (squares) or reflectance (spheres) measurement. **b)** The correlation of the relative reflectance and ratiometric UCNP emission. R^2 of the linear fitting was > 0.99. Error bars represent standard deviation.

There is reason to believe that the nanosized particles are moving along with the sample towards the bottom of the sensing layer. Therefore a part of the detected UCNP emission doesn't travel through the sensing layer, thus preventing an efficient attenuation of the UV-emission by the indicator and limiting the assay sensitivity. This issue needs to be studied further in order to develop more precise and reliable assays. Either the particles and indicator will have to be immobilized in separate layers in order to have efficient filtering of the signal or they could be brought to a close proximity in order to establish an energy transfer between them.

The low UV-emission intensity of the UCNP requires the use long integration times in the detection, lowering the kinetic resolution of the assay. In order to gather more of the emission light, one possibility would be to redesign the test strip in a format that would enhance the UCNP emission as described by Kuningas et al[30] who reported an enhancement in the UCP emission when using white microtiter wells instead of transparent ones.

Nevertheless the process of producing UV emission from NIR excitation consumes a lot of excitation photons as it's only possible to produce 1 UV photon per 3.7 NIR photons. Interesting alternative might be the materials that produce UV emission with a VIS-excitation demonstrated by e.g. Kumar and Rai[31]. They used tellurite glass doped with Nd^{3+} and Pr^{3+} ions and produced UV-emission with 532 nm excitation. In this case a single UV photon requires only two excitation photons.

Experimental

Reagents and instrumentation

Yttrium, ytterbium and thulium chloride hexahydrate ($RCl_3 \cdot 6H2O$, 99.99 %), ammonium fluoride (NH_4F, ≥ 99.99 %), sodium hydroxide (NaOH, ≥ 98 %) and potassium hydroxide (KOH, 99.99 %) were supplied by Sigma-Aldrich and used as starting materials without further purification. The purities of the rare earth chlorides are with respect to other lanthanides.

To identify the crystallization phase X-ray powder diffraction (XRD) analysis was carried out using a Huber G670 image plate Guinier camera (2θ range: 4-100°) with copper Kα1 radiation (λ: 1.5406 Å). The size and morphology of nanocrystals were characterized by transmission electron microscopy (Tecnai12 BioTwin TEM) with an acceleration voltage of 120 kV. The effect of K^+ in the UCP lattice on the UV-emission intensity was studied with a Varian Cary Eclipse fluorescence spectrophotometer (Varian Scientific Instruments, Mulgrave, Australia) equipped with a near-infrared (NIR) laser diode module C2021-F1 (Roithner Lasertechnik, Vienna, Austria) with emission at 980 nm.

The following components were used for the dry chemistry test strips: Sipernat FK 320DS (Evonik Industries AG, Hanau, Germany), poly(acrylic acid, sodium salt) (average molecular weight ~15 000, Sigma-Aldrich, Steinheim, Germany), Gantrez S-97 BF (Ashland, Marl, Germany), Propiofan 70D (BASF, Ludwigshafen, Germany), Geropon T77 (Rhodia, Milan, Italy) and ZrO_2 TZ-3YS (Tosoh Corporation, Kaisei-cho, Japan). Carba-nicotinamide adenine dinucleotide (cNAD) and modified glucose dehydrogenase were both produced in the company (Roche Diagnostics GmbH, Penzberg, Germany). The

supporting plastic film was Bayfol CR210 (125 µm thick, Bayer MaterialScience AG, Leverkusen, Germany).
The samples used in the glucose assay were either glucose in water (anhydrous β-D-glucose, Merck KGaA, Darmstadt, Germany) in concentrations ranging from 0-44.4 mM or a pooled sample of heparinized whole blood from multiple voluntary donors spiked with glucose.
The test strips were measured with a J&M spectrometer with an internal 35 W deuterium light source (Tidas S DAD, J&M Analytik AG, Essingen, Germany) together with KG5 bandpass filter (FGS600, Thorlabs, Munich, Germany) using a 100 mW NIR-laser for the excitation of UCNPs (RLD-0980-PFR LabSpec 980 nm, Laserglow technologies, Toronto, Canada). An additional KG5 filter was added when exciting the UCNPs through the sample The optical output from the laser entering the test strip was measured with an Advantest TQ8210 optical power meter with Q82017A sensor (Advantest Europe GmbH, Munich, Germany).

Nanocrystal synthesis

The synthesis of UV-emitting nanocrystalline β-$Na_{1-x}K_xYF_4$:Yb^{3+},Tm^{3+} materials, has been carried out in the presence of various K^+ concentrations ranging from 0 to 100 mol%, by a coprecipitation method according to a previously published procedure[32]. In a typical synthesis, 0.2 M RCl_3 (R:Y (4.77 mL), Yb (1.20 mL) and Tm (0.03 mL) total volume of rare-earth chloride solution was 6 mL) in methanol were added to a 250 mL two neck round-bottom flask containing 9 mL oleic acid (OA) and 21 mL 1-octadecene (ODE). The solution was magnetically stirred and heated to 160 °C under flowing argon for 40 min and then cooled down to room temperature. Thereafter, 15 mL methanol solution of NH_4F (4.8 mmol) and 100-x % NaOH + x % KOH (x = 0-100, total 3 mmol) was added and solution was stirred for 30 min without argon. The temperature was then increased to 310 °C under argon for 90 min. After the solution was slowly cooled down at room temperature, absolute ethanol was added to the reaction solution to precipitate the nanocrystals. The solution was then transferred to the centrifuge tube and centrifuged at 3 766 g for 8 min. The particles were washed 6 times like this with ethanol. To remove oleic acid from the particle surface, UCNPs were dissolved in 0.1 M HCl (pH 1) and incubated for 5 hours. After incubation, methanol and isopropanol (in the ratio of 10:3) were added into the solution. The pellet was collected by centrifugation, washed once with toluene, and finally dispersed in methanol.

Preparation of the dry chemistry layers

The general structure of the test strips is presented previously[33, 34]. The dry chemistry layer on the test strips were composed of two layers, a bottom one with the sensing elements (enzyme and the indicator), and a top one with the UCNP. The coating masses were prepared by dissolving/suspending the different components in mQ-water. Homogenous distribution was ensured by mechanical stirring, sonication and pressing the mixture through a fine mesh cloth. The composition of the bottom layer was 101.1 g L^{-1} Sipernat FK 320DS, 8.1 g L^{-1} polyacrylic acid, 15.3 g L^{-1} Gantrez, 40.4 g L^{-1} Propiofan 70D, 1.6 g L^{-1} Geropon T77, 64.7 g L^{-1} cNAD and 32.3 g L^{-1} glucose dehydrogenase with pH adjusted to 7.5.
For the upper layer the UCNP-particles were bound with the Gantrez polymer by first preparing a solution with 20 mg mL^{-1} Gantrez and 92 mg mL^{-1} UCNP in methanol. After the polymer had dissolved, water was added and pH adjusted with NaOH while mixing until a homogeneous suspension was formed. Methanol was then removed with a rotary evaporation and water was added to obtain the final concentrations of 65 g L^{-1} Gantrez and 300 g L^{-1} of UCNP. This mixture was then combined with the rest of the dry layer components in the final concentrations of 411.6 g L^{-1} ZrO_2, 8.7 g L^{-1} polyacrylic acid, 54.1 g L^{-1} Propiofan 70D and 1 g L^{-1} Geropon T77.
The coating masses were then spread on the plastic film using a manual blade coating. The first layer, containing the enzyme and the indicator, was coated with a blade height of 75 µm and dried in a drying oven at +35 °C for 15 minutes. After this, the second layer containing the UCNP was applied on top of this with a blade height of 100 µm from the film and dried the same way.

Measurement and analysis

Figure 6 a shows the structure of a glucose sensing test strip incorporating the UCNPs. Glucose measurement on the strip was based on the reduction of cNAD to cNADH as a result glucose reacting with the glucose dehydrogenase enzyme[35-37]. As a result of the reduction, the UV-absorption of the indicator increases in a region that matches perfectly with the UV-emission of the UCNP. Figure 6 shows the absorption spectra of cNAD and cNADH together with the UCNP emission from 300 to 550 nm. The blue emission of the UCNP around 475 nm remains unaffected in the measurement and can be used as a control signal.

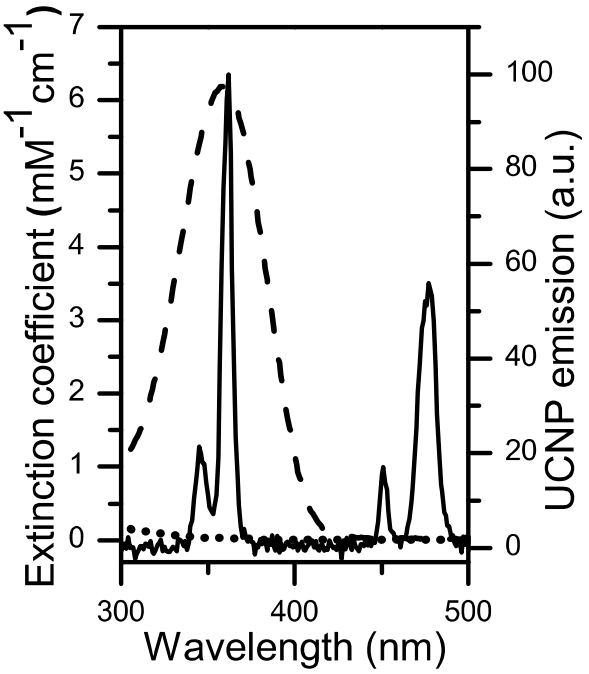

Figure 6. The absorption spectra of the cNAD (dotted line) and cNADH (dashed line) together with the UCNP emission (solid line).

The amount of cNADH formed on the strip was determined by directing a NIR-laser or broadband light source to the test strip

from below (the supporting film side) and detecting the decrease in the UV-radiation (originating either from the UCNPs or the reflection from the sensing layer) in a 45° angle (Figure 5 b left side). The laser power entering the test strip was 2,4 W cm^{-2}. For UCNPs also alternative detection setup was tested together with the spiked whole blood sample. In this the laser was pointed to the test strip from the sample side with the power of 9.1 W cm^{-2}, having the excitation travel through the layer of blood, and the emission was detected on the film side straight below (Figure 5 b right side). For this measurement a second identical KG5 filter was used to protect the detector from the laser. Total of five replicates were measured with each of the methods.

The UCNP emission and the reflectance were both recorded from 300-1000 nm with an integration time of 550 ms with 5x spectrum accumulation. The total measurement time and exposure to the excitation was 45 s. Same strips were used in all measurements. The spectrum was recorded initially from a dry strip without any sample to obtain the reference signal and subsequently, after the addition of the 5 µL sample of either glucose in water or whole blood spiked with glucose, with three second intervals.
From each of the UCNP emission spectra, the background subtracted 330-380 nm (I_{UV}) and 440-490 nm (I_{ctrl}) peaks were integrated and used to calculate the ratiometric signal I_{UV}/I_{ctrl}. The emission from 440-490 nm was chosen as a control as it is spectrally close to the UV-peak and unaffected by the absorption of the indicator compound. Ratiometric signal compensates for the fluctuation caused by factors including quenching from the wetting of the test strip, and also potential heating of the UCNPs by the excitation. In the case of reflectance, intensity at 362 nm was used. The reaction endpoint was determined as a point where the slope of the kinetic curve was < 2 %/s. In order to compare the two methods, the value in the endpoint was represented as a relative signal determined as a percentage of the respective signal obtained from the dry strip, before the addition of a sample. The limit of detection was calculated as the point on the calibration curve, that deviates from the zero sample by three standard deviations. Origin 8.0.6 (OriginLab Corporation, Northampton, United States) was used to calculate the root-mean-square error.

Conclusions

In this paper we presented the utilization of UV-emitting upconverting nanophosphors as an internal light source in glucose sensing test strips and compared the feasibility of this approach against the use of external UV light source. As reflectance measurement is sensitive to various parameters (such as the intensity and the angle of the incident light and the angle of the detection), UCNPs provide an alternative detection method with a greater degree of freedom in the detection setup. The combination of the penetration depth of the NIR-excitation and the internal control signal offer advantages unachievable with many other optical methods. The results from the UCNP measurement showed a good correlation with the reflectance measurement.

Acknowledgements
This research was supported by the European Union under Grant Agreement number 264772 (ITN CHEBANA).

Notes and references

[a] Roche Diagnostics GmbH, Sandhofer Straße 116, 68305 Mannheim, Germany.
[b] University of Turku, Department of Biotechnology, Tykistökatu 6 A 6th floor, 20520 Turku, Finland.
† These authors contributed equally to this work.

Electronic Supplementary Information (ESI) available: [details of any supplementary information available should be included here]. See DOI: 10.1039/b000000x/

1. M. Haase and H. Schafer, *Angew Chem Int Ed Engl*, 2011, **50**, 5808-5829.
2. X. Chen, W. Wang, X. Chen, J. Bi, L. Wu, Z. Li and X. Fu, *Materials Letters*, 2009, **63**, 1023-1026.
3. W. Huang, M. Ding, H. Huang, C. Jiang, Y. Song, Y. Ni, C. Lu and Z. Xu, *Materials Research Bulletin*, 2013, **48**, 300-304.
4. T. Jiang, W. Song, S. Liu and W. Qin, *Journal of Fluorine Chemistry*, 2012, **140**, 70-75.
5. X. Liu, R. Dai, Z. Wang and Z. Zhang, *Journal of Rare Earths*, 2010, **28, Supplement 1**, 215-218.
6. Y.-F. Wang, L.-D. Sun, J.-W. Xiao, W. Feng, J.-C. Zhou, J. Shen and C.-H. Yan, *Chemistry – A European Journal*, 2012, **18**, 5558-5564.
7. C.-J. Carling, J.-C. Boyer and N. R. Branda, *J Am Chem Soc*, 2009, **131**, 10838-10839.
8. B. F. Zhang, M. Frigoli, F. Angiuli, F. Vetrone and J. A. Capobianco, *Chem Commun (Camb)*, 2012, **48**, 7244-7246.
9. C.-J. Carling, F. Nourmohammadian, J.-C. Boyer and N. R. Branda, *Angewandte Chemie International Edition*, 2010, **49**, 3782-3785.
10. M. K. G. Jayakumar, N. M. Idris and Y. Zhang, *Proceedings of the National Academy of Sciences*, 2012, **109**, 8483-8488.
11. B. Yan, J.-C. Boyer, N. R. Branda and Y. Zhao, *J Am Chem Soc*, 2011, **133**, 19714-19717.
12. B. Yan, J.-C. Boyer, D. Habault, N. R. Branda and Y. Zhao, *J Am Chem Soc*, 2012, **134**, 16558-16561.
13. Y. Yang, Q. Shao, R. Deng, C. Wang, X. Teng, K. Cheng, Z. Cheng, L. Huang, Z. Liu, X. Liu and B. Xing, *Angewandte Chemie International Edition*, 2012, **51**, 3125-3129.
14. L. L. Fedoryshin, A. J. Tavares, E. Petryayeva, S. Doughan and U. J. Krull, *ACS applied materials & interfaces*, 2014, **6**, 13600-13606.
15. S. Beyazit, S. Ambrosini, N. Marchyk, E. Palo, V. Kale, T. Soukka, B. Tse Sum Bui and K. Haupt, *Angewandte Chemie International Edition*, 2014, **53**, 8919-8923.
16. R. Ali, S. M. Saleh, R. J. Meier, H. A. Azab, I. I. Abdelgawad and O. S. Wolfbeis, *Sensors and Actuators B: Chemical*, 2010, **150**, 126-131.
17. H. S. Mader and O. S. Wolfbeis, *Analytical chemistry*, 2010, **82**, 5002-5004.
18. L.-N. Sun, H. Peng, M. I. J. Stich, D. Achatz and O. S. Wolfbeis, *Chem Commun (Camb)*, 2009, 5000-5002.
19. D. E. Achatz, R. J. Meier, L. H. Fischer and O. S. Wolfbeis, *Angewandte Chemie International Edition*, 2011, **50**, 260-263.
20. M. del Barrio, S. de Marcos, V. Cebolla, J. Heiland, S. Wilhelm, T. Hirsch and J. Galbán, *Biosensors and Bioelectronics*, 2014, **59**, 14-20.
21. S. Wilhelm, M. Del Barrio, J. Heiland, S. F. Himmelstoss, J. Galban, O. S. Wolfbeis and T. Hirsch, *ACS applied materials & interfaces*, 2014, **6**, 15427-15433.
22. V. Kale, T. Soukka, J. Hölsä and M. Lastusaari, *Journal of Nanoparticle Research*, 2013, **15**, 1-12.

23. S. Zeng, G. Ren, W. Li, C. Xu and Q. Yang, *The Journal of Physical Chemistry C*, 2010, **114**, 10750-10754.
24. J.-C. Boyer, M.-P. Manseau, J. I. Murray and F. C. J. M. van Veggel, *Langmuir*, 2010, **26**, 1157-1164.
25. A. D. Ostrowski, E. M. Chan, D. J. Gargas, E. M. Katz, G. Han, P. J. Schuck, D. J. Milliron and B. E. Cohen, *ACS Nano*, 2012, **6**, 2686-2692.
26. J. Shen, G. Chen, T. Y. Ohulchanskyy, S. J. Kesseli, S. Buchholz, Z. Li, P. N. Prasad and G. Han, *Small*, 2013, **9**, 3213-3217.
27. F. Vetrone, R. Naccache, V. Mahalingam, C. G. Morgan and J. A. Capobianco, *Advanced Functional Materials*, 2009, **19**, 2924-2929.
28. F. Wang, J. Wang and X. Liu, *Angewandte Chemie International Edition*, 2010, **49**, 7456-7460.
29. G.-S. Yi and G.-M. Chow, *Chemistry of Materials*, 2007, **19**, 341-343.
30. K. Kuningas, T. Rantanen, T. Lövgren and T. Soukka, *Analytica Chimica Acta*, 2005, **543**, 130-136.
31. K. Kumar and S. B. Rai, *Solid State Communications*, 2007, **142**, 58-62.
32. V. Kale, T. Soukka, J. Hölsä and M. Lastusaari, *Journal of Nanoparticle Research*, 2013, **15**, 1-12.
33. *US Pat.*, 7629175, 2009.
34. *EP Pat.*, 0821233, 2002.
35. *WO Pat.*, 103540, 2009.
36. *WO Pat.*, 012494, 2007.
37. J. T. Slama and A. M. Simmons, *Biochemistry*, 1988, **27**, 183-193.